Applied Mathematics & Information Sciences
An International Journal

http://dx.doi.org/10.18576/amis/130201

Approximate Solutions to Lane-Emden Equation for Stellar Configuration

Fazal Abbas[1,*], *Petko Kitanov*[2] *and Shoshanna Longo*[3]

[1] Department of Mathematics and Computer Sciences, Stetson University, Florida, USA
[2] School of Mathematical Sciences, Rochester Institute of Technology, New York, USA
[3] Computer Engineering, Rochester Institute of Technology, New York, USA

Received: 22 Dec. 2018, Revised: 21 Jan. 2019, Accepted: 24 Jan. 2019
Published online: 1 Mar. 2019

Abstract: In this paper, we consider the Lane-Emden equation of the first kind which arises in the study of stellar structures. We use multiple algorithms, based on Homotopy Analysis Method (HAM) to find the convergent series solutions to the singular, non-linear, initial value problem. It is found that the radius of convergence for the solutions is affected by three factors: the choice of initial value, the order and type of non-linearity, and the linear operator used. We then compare analytical results to the 20^{th} order series solution, the Pade approximant to the series, and the approximate solution obtained via the Runge-Kutta-Fehlberg method (RKF45).

Keywords: Lane-Emden equation, stellar configuration, Homotopy Analysis Method, Runge-Kutta-Fehlberg method, Pade approximant

1 Introduction

Astrophysicist J. Homer Lane derived and studied an equation that models the equilibrium of stellar configurations in [7]. Later, Emden extended this work in [6]. This is known as the Lane-Emden equation that describes the polytropic models and can be written as

$$x^{-2}\frac{d}{dx}\left(x^2\frac{dy}{dx}\right)+y^M=0. \tag{1}$$

Where y^M is the polynomial non-linearity, and M is a constant whose value depends on the physical phenomena modeled by (1). With the inclusion of polynomial non-linearity, (1) can be used to model spherical clouds of gas. While the behavoir of such clouds is subject to laws of thermodynamics. Furthermore, if the form of the non-linearity is changed from y^M to e^y, then (1) yields the Lane-Emden equation.

To derive the Lane-Emden equation we start with the equation of hydrostatic equilibrium

$$\frac{r^2}{\rho}\frac{dP}{dr}=-GM_r. \tag{2}$$

where P is pressure, ρ is density, M_r is the mass of a ball with radius r, and G is the gravitational constant. Taking the derivative with respect to r and expressing the mass in terms of density and volume, we obtain

$$\frac{1}{r^2}\frac{d}{dr}\left(\frac{r^2}{\rho}\frac{dP}{dr}\right)=-4\pi G\rho. \tag{3}$$

We seek solution in the form $P(\rho)=K\rho^a$, where K and a are constant. Using this substitution, (3) becomes as follows;

$$\frac{Ka}{r^2}\frac{d}{dr}\left(r^2\rho^{a-2}\frac{d\rho}{dr}\right)=-4\pi G\rho. \tag{4}$$

Let $a=(M+1)/M$, where M is the polytropic index. We introduce a new variable y by $\rho(r)=\rho_c[y(r)]^M$, where $0\le y\le 1$ allows (4) to be written as

$$\left[(M+1)\frac{K\rho^{(1-M)/M}}{4\pi G}\right]\frac{1}{r^2}\frac{d}{dr}\left[r^2\frac{dy}{dr}\right]=-y^M. \tag{5}$$

Introducing a new constant $l_M^2=\left[(M+1)\frac{K\rho^{(1-M)/M}}{4\pi G}\right]$ and rescaling the variable r by $r=l_Mx$ the equation (5) simplifies to

$$\frac{1}{x^2}\frac{d}{dx}\left[x^2\frac{dy}{dx}\right]=-y^M. \tag{6}$$

* Corresponding author e-mail: fabbas1@stetson.edu

Equation (6) then simplifies to the standard Lane-Emden equation.
The Lane-Emden equation has been widely studied. While Chandrasekhar [5] and Carroll [4] were the first to model and study the Lane-Emden equation analytically. Several analytical studies for these types of equations using the Adomian Decomposition Method (ADM) have been presented in [3], [18], [22], [25], [19]. Variational Iteration Method (VIM) has also been used in [24], [23], [19], [17] to study the Lane-Emden-Fowler-type of equations. Homotopy Perturbation Method(HPM) which is another choice of finding the convergent series solution to non-linear problems has been used in [12] to study the Lane-Emden equation. In [14], [15], [13], [2] the authors indicate that HPM may not always be an excellent choice for solving problems with strong non-linearity. In [1] the authors also used the HPM approach to find the analytical solution to a diffusive flux study for the biofilm modeling and found the same challenge as proposed in [14].
Liao in his doctoral thesis [11], proposed a new analytical approach named Homotopy Analysis Method (HAM). HAM is based on the idea of topology. The focus of the HAM scheme is to transform a given non-linear differential equation into several linear differential equations, and then to combine the solutions to develop an infinite series of the actual solution. In [16], [10], [9], [8] the HAM approach is applied to find the convergent series solution to Lane-Emden-type equations. In [16] an analytical solution to the standard second-order Lane-Emden initial value problem of the first kind is presented. They compared the HAM series solution with the traditional power series solution. They found that HAM gives a larger interval of convergence than that of the power series solution. In this current study, we employ a variety of algorithms based on HAM. The solutions generated by these HAM algorithms are then compared to the Pade series solution. We observe that the HAM algorithms are faster, and they achieve a larger interval of convergence than the interval presented by the authors in [16].
This paper is organized as follows;
In section 2, we compare the 20^{th} order power series solution and its Pade approximant with the numerical solution. The Pade approximant gives the larger and faster interval of convergence than the traditional power series solution. We show that an increase in the initial value and an increase in the value of M reduces the radius of convergence. In Section 3, we present the detailed proof of obtaining various HAM algorithms, showing that $H_1(x;p)$ has the largest interval of convergence. We notice that the auxiliary parameter $\hbar$ in the construction of HAM algorithm plays a vital role in finding the convergent solution with the largest radius of convergence.

2 Analysis via Pade Approximant on Power Series

We start with the standard second-order Lane-Emden initial value problem:

$$x^{-2}\frac{d}{dx}\left(x^2\frac{dy}{dx}\right)+y^3(x)=0; \quad y(0)=a, y'(0)=0 \quad (7)$$

The Pade approximant on a series solution is a useful technique to increase the radius of convergence for the solution of non-linear problems. In the figures 1(a-c): we plot the numerical comparison for the 20^{th} order power series solution to its Pade approximant. It is important to note that an increase in the initial value a decreases the radius of convergence overall.

Observing the case when $a = 1$ in figure 1(a): the power series solution diverges from the values greater than 2.32, while its Pade approximant diverges from the values greater than 6.66. Considering the situation when $a = 5$ in figure 1(b), the power series solution diverges from the values greater than 1.28, while its Pade approximant diverges from the values greater than 0.44. The power series solution diverges from the values greater than 0.66 in figure 1(c) for $a = 10$, while its Pade approximant diverges from the values greater than 0.22. The plots in figures 1(a-c) show an approximate three-fold increase in the interval of convergence.

We look at the effects of increasing values of M in y^M on the interval of convergence for the solution of a Lane-Emden equation and we also analyze the whole situation with changing initial values in the model. For this purpose, we compare the 20^{th} order Pade approximant with RKF45, a numerical scheme.

In the figures 2(a-c), we plot the Pade approximant to a 20^{th} order power series for increasing non-linearities $M = 3,4,5,6$ with initial values $a = 1$, $a = 5$ and $a = 10$ respectively. Looking at the case when $a = 1$ in figure 2(a), there is a one-fourth reduction in the interval of convergence from $(0,6.50)$ for $M = 3$ to $(0,1.35)$ for $M = 6$. Considering the situation when $a = 5$ in 2(b) where Pade series solution for $M = 3$ starts diverging at 1.28 and for the higher non-linearities $M = 4,5,6$, the Pade solution never converges to the actual solution. Observing the case when $a = 10$ in 2(b) where the Pade series solution for $M = 3$ starts diverging at 0.64 and for the higher non-linearities $M = 4,5,6$,it never converges to the actual solution.

3 HAM Algorithm for the Lane-Emden Initial Value Problem

3.1 Basic Idea of HAM

The idea of homotopy comes from topology. Homotopic equations for the non-linear problems provide a mapping,

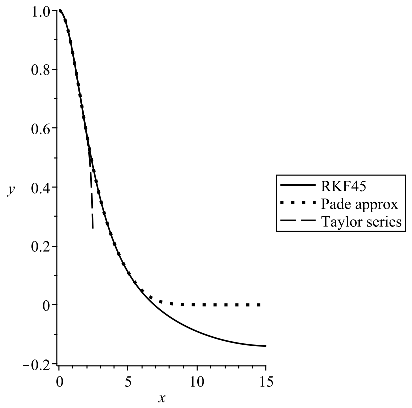

(a) Taylor series solution vs its Pade approximant for $a = 1$

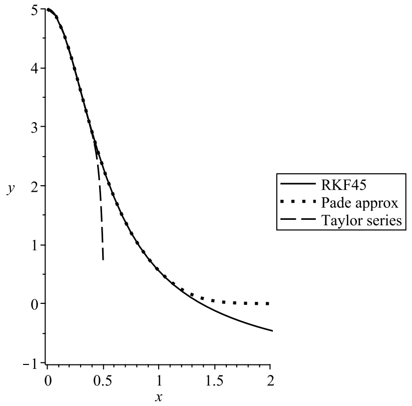

(b) Taylor series solution vs its Pade approximant for $a = 5$

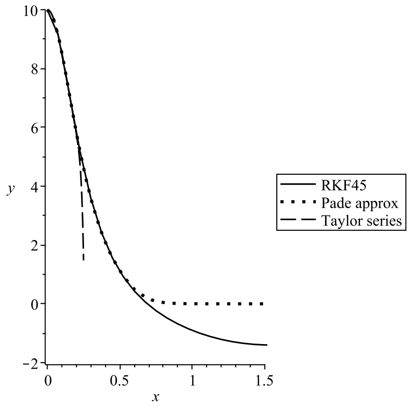

(c) Taylor series solution vs its Pade approximant for $a = 10$

Fig. 1: Numerical comparison for the Lane-Emden model with the 20^{th} order power and its Pade approximant when $a = 1$ in (a) when $a = 5$ in (b) and when $a = 10$ in (c).

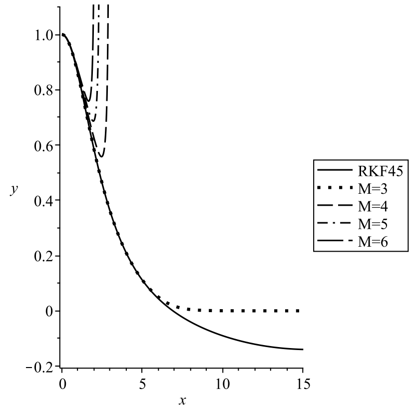

(a) non-linearity analysis for Pade approximant with $a = 1$

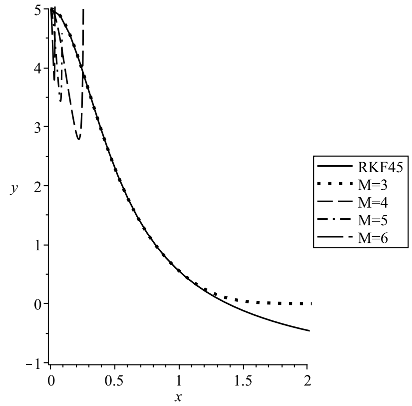

(b) non-linearity analysis for Pade approximant with $a = 5$

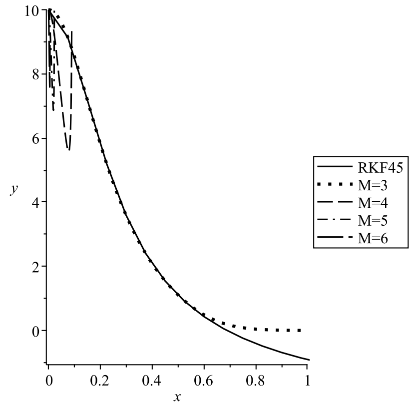

(c) non-linearity analysis for Pade approximant with $a = 10$

Fig. 2: Numerical comparisons of the model with Pade approximant when $a = 1$ for increasing non-linearities M in (a) when $a = 5$ for increasing non-linearities M in (b) and when $a = 10$ for increasing non-linearities M in (c).

starting from an initial guess to the actual solution of the problem. Homotopy Analysis Method (HAM) does not even require a small parameter in the model. Moreover, it transforms a non-linear problem into a recursive sequence of linear problems which are comparitvely easy to solve. Adding the solutions of linear problems provides an approximate convergent series solution of the model. It is always interesting to use the HAM approach to problems not having the exact solution. So the numerical comparison, in this case, is helpful to visualize the rate of convergence for HAM approximation.

The selection of the linear operator in the construction of the homotopy equation and the value of auxiliary parameter $\hbar$ in the homotopy equation plays an essential role in finding a quick convergent series solution. Additionally, we name the auxiliary parameter $\hbar$ as a convergence controlling agent, as it helps to not only obtain a convergent solution but also to enhance the interval of convergence.

We define for $p \in [0,1]$ the homotopy as

$$H_1(x,p) := \\ (1-p)\mathscr{L}[v(x;p)-y_0(x)] = \hbar p\left[\mathscr{L}v(x;p)+v^3(x;p)\right], \\ v(0;p)=a, \quad v'(0;p)=0. \tag{8}$$

Where

$$\mathscr{L}[v] = x^{-2}\frac{\partial}{\partial x}\left(x^2\frac{\partial}{\partial x}\right)[v]$$

It is easy to verify that for $p=1$ this is equivalent to (7). Moreover, every function that satisfies the boundary conditions is a valid solution of (8) for $p=0$. We expand $v(x;p)$ in a power series about $p=0$ to obtain

$$v(x;p) = v(x;0) + \sum_{m=0}^{+\infty}\left(\frac{v^{(m)}(x;p)|_{p=0}}{m!}\right)p^m. \tag{9}$$

Sufficient regularity is formally provided in the problem to support series convergence, therefore,

$$v(x;1) = v(x;0) + \sum_{m=0}^{+\infty}\frac{v^{(m)}(x;p)|_{p=0}}{m!}. \tag{10}$$

We call the terms under the sum the mth-order deformation derivative, defined as

$$y_m(x) := \frac{v^{(m)}(x;p)|_{p=0}}{m!}.$$

The solution of (7) is then

$$y(x) = y_0 + \sum_{m=1}^{+\infty} y_m(x), \tag{11}$$

where $y_0(x) = v(x;0)$ and $y_m(x)$ is the mth-order approximation to the actual solution. It is expected in general that the mth-order approaches the actual solution. However, several problems in the literature require only a few terms of HAM solution to compare with their closed form solution.

3.2 Recursive Linear Algorithm for $H_1(x;p)$

The deformation derivatives can be computed in analogy to the theory summarized in [8]. For our specific problem, the following algorithm applies.

Theorem 3.1. *For $y_0 = a$, the deformation derivative y_m associated with homotopy H_1 are obtained recursively as solutions of the initial value problem*

$$\mathscr{L}[y_m(x)] = (\hbar+\chi_m)\mathscr{L}[y_{m-1}(x)] + \hbar[\sum_{k=0}^{m-1} y_{m-1-k}\sum_{l=0}^{k} y_l y_{k-l}] \\ y_m(0)=a, y'_m(0)=0, \tag{12}$$

where

$$\mathscr{L}[\cdot] = x^{-2}\frac{d}{dx}\left(x^2\frac{d}{dx}\right)[\cdot].$$

Moreover,

$$\chi_m = \begin{cases} 1 & m \le 1 \\ 0 & m > 1 \end{cases}$$

Proof. Substituting (9) into (8) and applying Leibniz' Rule, we obtain for the left-hand side of (8)

$$L.H.S = \sum_{l=0}^{m}\binom{m}{l}(1-p)^{(l)}\mathscr{L}[v(x;p)-y_0(x)]^{(m-l)} \\ = m!\mathscr{L}\left[\frac{v^{(m)}(x;p)|_{p=0}}{m!} - \frac{v^{(m-1)}(x;p)|_{p=0}}{(m-1)!}\right] \\ = m!\mathscr{L}[y_m(x) - \chi_m y_{m-1}(x)]$$

also, for the right-hand side of (8), we have

$$\sum_{l=0}^{m}\binom{m}{l}(\hbar p)^{(l)}\left[\mathscr{L}v(x;p)+v^3(x;p)\right]^{(m-l)} \\ = m!\hbar\left[\mathscr{L}\left(\frac{v^{(m-1)}(x;p)|_{p=0}}{(m-1)!}\right)\right. \\ \left. + \sum_{k=0}^{m-1}\frac{v^{(m-1-k)}(x;p)|_{p=0}}{(m-1-k)!}\sum_{l=0}^{k}\frac{v^{(l)}(x;p)|_{p=0}}{l!}\frac{v^{(k-l)}(x;p)|_{p=0}}{(k-l)!}\right] \\ = m!\hbar\left[\mathscr{L}y_{m-1}(x) + \sum_{k=0}^{m-1} y_{m-1-k}(x)\sum_{l=0}^{k} y_l(x)y_{k-l}(x)\right]$$

Thus, for the mth-deformation derivative we obtain with the initial conditions in (8) the recursive linear initial value problem as follows;

$$\mathscr{L}[y_m(x)] = (\hbar+\chi_m)\mathscr{L}[y_{m-1}(x)] + \hbar[\sum_{k=0}^{m-1} y_{m-1-k}\sum_{l=0}^{k} y_l y_{k-l}] \\ y_m(0)=a, y'_m(0)=0$$

□

3.3 Numerical Comparison with HAM for the Lane-Emden IVP

HAM algorithm is based on the fact that the auxiliary parameter $\hbar$, used in constructing the homotopy equation, not only controls the interval of convergence but also helps in finding the convergent series solution of the problem.

We present a numerical comparison of model with various choices of auxiliary parameter values $\hbar = -0.09, -0.12, -0.15$ for the 20^{th} order HAM solution based on the homotopy construction defined in (8). It is shown in the figures 5(a-c) that $\hbar$ controls the interval of convergence with various choices of the initial values $a = 1, 5, 10$. Additionally, the increasing values of a in figures 5(a-d) reduce the interval of convergence in general. In figure 5(a) with $a = 1$, we have the interval of convergence for $\hbar = -0.09$ $(0, 10.80)$, $\hbar = -0.12$ $(0, 9.50)$ and $\hbar = -0.15$ $(0, 8.27)$. In figure 5(b) with $a = 5$, we observe the maximum interval of convergence for $\hbar = -0.09$ which is $(0, 1.10)$. Lastly, in figure 5(c) with $a = 10$, we observe the maximum interval of convergence for $\hbar = -0.09$ which is $(0, 2.25)$.

We present the numerical comparison between the 30^{th} order power series, Pade approximant on it and 20^{th} order HAM series solution. It is shown in the figures 3(a-c) that HAM converges faster and has a bigger interval of convergence with various choices of the initial values $a = 1, 5, 10$ than the traditional power series solution and its associated Pade series. Moreover, increasing the initial value reduces the interval of convergence in general. In figure 3(a) with $a = 1$, we compare the 20^{th} order HAM series, 30^{th} order power series and Pade approximant with RKF45. We notice that the interval of convergence for HAM $(0, 10.60)$, power series $(0, 2.21)$ and Pade solution $(0, 5.36)$. It is observed that HAM achieves a bigger interval of convergence with the substantial small number of approximations that we obtained in the case of power series and its Pade approximant. In figure 3(c) with $a = 5$, we have the interval of convergence for HAM, power and Pade as $(0, 2.20)$, $(0, 0.44)$ and $(0, 1.05)$ respectively. finally, in figure 3(c) with $a = 10$, the interval of convergence for HAM, power and Pade are $(0, 1.07)$, $(0, 0.23)$ and $(0, 0.51)$ respectively. It is important to note that with the increasing initial values, HAM interval of convergence is significantly larger than the traditional series method.

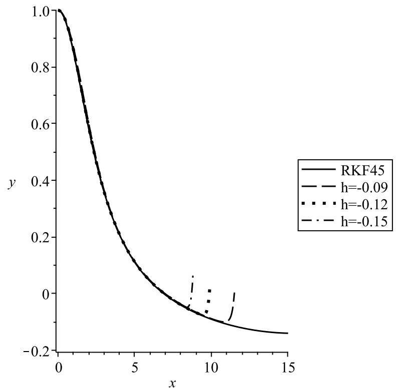

(a) HAM series solution of the model for $a = 1$

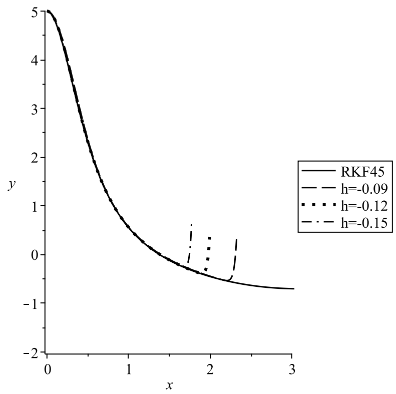

(b) HAM series solution of the model for $a = 5$

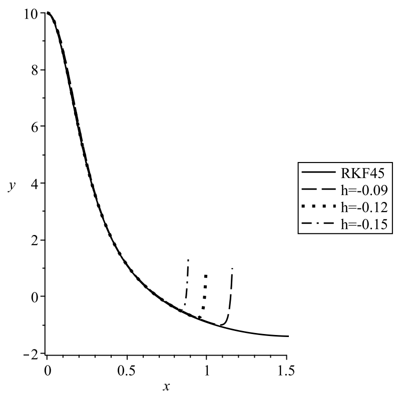

(c) HAM series solution of the model for $a = 10$

Fig. 3: Numerical comparison with the 20^{th} order HAM series solution for differenent values of auxiliary parameter $\hbar$ when $a = 1$ in (a), when $a = 5$ in (b) and when $a = 10$ in (c).

3.4 Other Possible HAM Algorithms for the Lane-Emden IVP

We define for $p \in [0, 1]$ the homotopy

$$\begin{aligned} H_2(x, p) &:= (1-p)\mathscr{L}[v(x;p) - y_0(x)] \\ &= \hbar p \left[\mathscr{L}v(x;p) + \tfrac{2}{x}\tfrac{\partial v(x;p)}{\partial x} + v^3(x;p)\right], \\ v(0;p) &= a, \quad v'(0;p) = 0, \end{aligned} \tag{13}$$

where

$$\mathscr{L}[v] = \frac{\partial^2}{\partial x^2}[v].$$

Theorem 3.2. *For $y_0 = a$, the deformation derivative y_m associated with homotopy H_2 are obtained recursively as solutions of the initial value problem*

$$\begin{aligned} &\mathscr{L}[y_m(x)] \\ &= (\hbar + x_m)\mathscr{L}[y_{m-1}(x)] + \hbar[\tfrac{2}{x}y_{m-1}^{(1)} + \sum_{k=0}^{m-1} y_{m-1-k} \sum_{l=0}^{k} y_l y_{k-l}] \\ &y_m(0) = a, y'_m(0) = 0, \end{aligned} \tag{14}$$

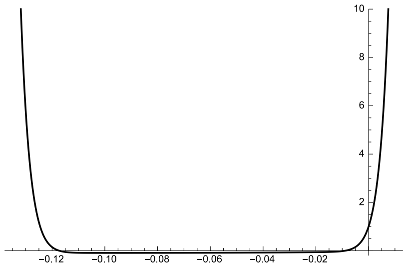

(a) h-curve for the HAM series solution with $a = 1$

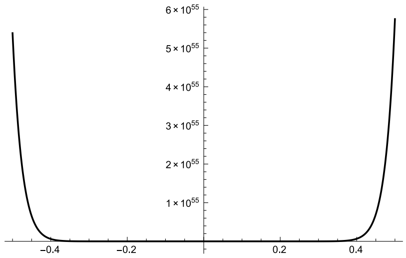

(b) h-curve for the HAM series solution with $a = 5$

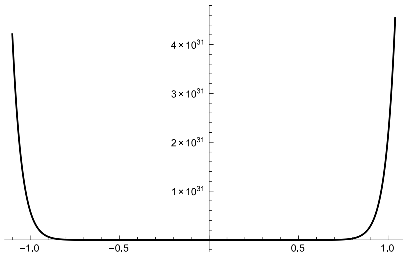

(c) h-curve for the HAM series solution with $a = 10$

Fig. 4: h-curve analysis for the 20^{th} order HAM series solution with $a = 1$ in (a), with $a = 5$ in (b) and with $a = 10$ in (c).

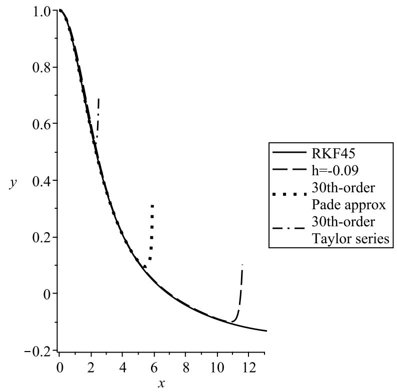

(a) solution comparison for Taylor, Pade and HAM when $a = 1$

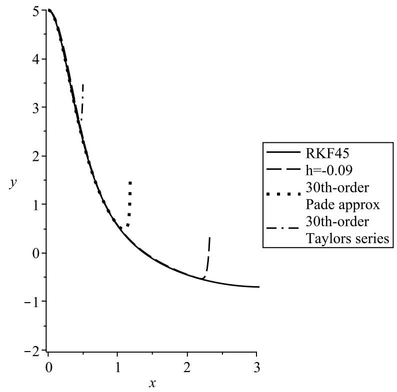

(b) solution comparison for Taylor, Pade and HAM when $a = 5$

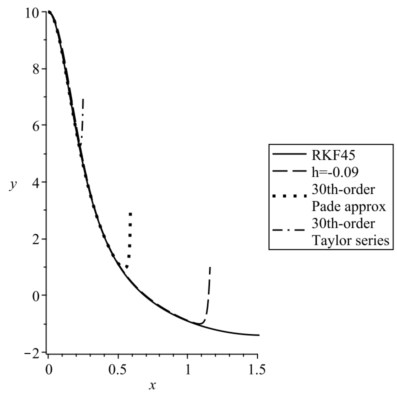

(c) solution comparison for Taylor, Pade and HAM when $a = 10$

Fig. 5: Numerical comparison with 30^{th} order power, its Pade approximant and 20^{th} order HAM series solution when $a = 1$ in (a), when $a = 5$ in (b) and when $a = 10$ in (c).

where

$$\mathscr{L}[\cdot] = \frac{d^2}{dx^2}[\cdot]$$

and

$$\chi_m = \begin{cases} 1 & m \leq 1 \\ 0 & m > 1. \end{cases}$$

Proof. Substituting (9) into (13) and applying Leibniz' Rule, we obtain for the left-hand side of (13)

$$\begin{aligned} L.H.S &= \sum_{l=0}^{m} \binom{m}{l} (1-p)^{(l)} \mathscr{L}[v(x;p) - y_0(x)]^{(m-l)} \\ &= m!\mathscr{L}\left[\frac{v^{(m)}(x;p)|_{p=0}}{m!} - \frac{v^{(m-1)}(x;p)|_{p=0}}{(m-1)!}\right] \\ &= m!\mathscr{L}[y_m(x) - \chi_m y_{m-1}(x)] \end{aligned}$$

so for the right-hand side of (13), we have

$$\sum_{l=0}^{m} \binom{m}{l} (\hbar p)^{(l)} \left[\mathscr{L}v(x;p) + \frac{2}{x}\frac{\partial v(x;p)}{\partial x} + v^3(x;p)\right]^{(m-l)}$$

$$= m!\hbar \left[\begin{array}{c} \mathscr{L}\left(\frac{v^{(m-1)}(x;p)|_{p=0}}{(m-1)!}\right) + \frac{2}{x}\frac{\partial}{\partial x}\left(\frac{v^{(m-1)}(x;p)|_{p=0}}{(m-1)!}\right) \\ + \sum_{k=0}^{m-1} \frac{v^{(m-1-k)}(x;p)|_{p=0}}{(m-1-k)!} \sum_{l=0}^{k} \frac{v^{(l)}(x;p)|_{p=0}}{l!} \frac{v^{(k-l)}(x;p)|_{p=0}}{(k-l)!} \end{array} \right]$$

$$= m!\hbar\left[\mathscr{L}y_{m-1}(x) + \frac{2}{x}y_{m-1}^{(1)} + \sum_{k=0}^{m-1} y_{m-1-k}(x)\sum_{l=0}^{k} y_l(x)y_{k-l}(x)\right]$$

Thus, for the mth-deformation derivative, we obtain with the initial conditions in (13) the recursive linear initial value problem.

$$\mathscr{L}[y_m(x)] = (\hbar + x_m)\mathscr{L}[y_{m-1}(x)] + \hbar[\tfrac{2}{x}y_{m-1}^{(1)} + \sum_{k=0}^{m-1} y_{m-1-k}\sum_{l=0}^{k} y_l y_{k-l}],$$
$$y_m(0) = a, y_m'(0) = 0$$

□

The next theorem justifies one more possible HAM algorithm. The proof of this theorem is similar to the proofs of the previous theorems, that is why it is omitted. We define for $p \in [0,1]$ the homotopy

$$H_3(x,p) := (1-p)\mathscr{L}[v(x;p) - y_0(x)] = \hbar p\left[\frac{\partial^2 v(x;p)}{\partial x^2} + \mathscr{L}v(x;p) + v^3(x;p)\right] = 0, \quad v(0;p) = a, \;\; v'(0;p) = 0. \tag{15}$$

where

$$\mathscr{L}[v] = \left(\frac{2}{x}\frac{\partial}{\partial x}\right)[v]$$

Theorem 3.3. *For $y_0 = a$, the deformation derivative y_m associated with homotopy H_2 are obtained recursively as solutions of the initial value problem*

$$\mathscr{L}[y_m(x)] = (\hbar + x_m)\mathscr{L}[y_{m-1}(x)] + \hbar[y_{m-1}^{(2)} + \sum_{k=0}^{m-1} y_{m-1-k}\sum_{l=0}^{k} y_l y_{k-l}] \quad y_m(0) = a, y_m'(0) = 0 \tag{16}$$

where

$$\mathscr{L}[\cdot] = \left(\frac{2}{x}\frac{d}{dx}\right)[\cdot]$$

and

$$\chi_m = \begin{cases} 1 & m \le 1 \\ 0 & m > 1. \end{cases}$$

□

3.5 Convergence Interval Analysis for Different HAM Algorithms

The choice of linear operator plays a vital role in the construction of the homotopy equation. The figures 6(a-c) show a numerical comparison of the choice of different HAM algorithms for the solution convergence of interval of the Lane-Emden model. We observe the same pattern that was seen before where the increasing initial values reduce the interval of convergence in general. Apart from that, all the plots in figures 6(a-c) show that it is possible to come up with a HAM algorithm with the largest radius of convergence.

Looking at the figure 6(a), we have intervals of convergence for HAM1 $(0,3.74)$, HAM2 $(0,5.53)$ and HAM3 $(0,10.70)$. Now considering the figure 6(b), we have intervals of convergence for HAM1 $(0,0.36)$, HAM2 $(0,0.54)$ and HAM3 $(0,1.07)$. Lastly, for figure 6(c), we have intervals of convergence for HAM1 $(0,0.72)$, HAM2 $(0,0.1.04)$ and HAM3 $(0,2.2)$

Now, we prove that the series (11) converges to the solution of the IVP. The proof is similar to the proof of the Banach fixed-point theorem. From our numerical simulations, we establish the fact that for two successive y_m and y_{m+1} we have the relation $\frac{||y_{m+1}||}{||y_m||} < 1$. Here $||.||$ denotes the usual sup norm. This means that there is constant c with $0 \le c < 1$, such that $||y_{m+1}|| \le c||y_m||$. We illustrate this fact in the next table, where several calculations are shown. The calculations are done for different values of the parameter a. The first row of the table shows the values of a and the corresponding intervals.

$c_m = \|\|y_{m+1}\|\|/\|\|y_m\|\|$	$a=1$; $[0,10.9]$	$a=5$; $[0,1.07]$	$a=10$; $[0,0.83]$
$c_1 = \|\|y_1\|\|/\|\|y_0\|\|$	0.178	0.597	0.882
$c_2 = \|\|y_2\|\|/\|\|y_1\|\|$	0.694	0.209	0.820
$c_3 = \|\|y_3\|\|/\|\|y_2\|\|$	0.714	0.816	0.424
$c_4 = \|\|y_4\|\|/\|\|y_3\|\|$	0.690	0.375	0.873
⋮	⋮	⋮	⋮
$c_{19} = \|\|y_{19}\|\|/\|\|y_{18}\|\|$	0.861	0.930	0.818
$c_{20} = \|\|y_{20}\|\|/\|\|y_{19}\|\|$	0.863	0.886	0.965

So, we have that $c_m < 1$ for all m. We can take $c = \sup_{m\in\mathbb{N}} s_m$
Taking into account this observation, we prove the following theorem.

Theorem 3.4. *If $||y_{m+1}|| \le c||y_m||$ with $0 \le c < 1$, then the series (11) converges to the solution of the corresponding solution of the IVP of the Lane-Emden equation.*

Proof. We need only to prove that the series (11) is convergent. The fact that the series converges to the solution of the considered IVP follows from a result proved by Liao in [9].

First, we note that all of our considerations are in the space of continuous functions defined on closed interval, namely the space $C[a,b]$ with the norm $||f|| = \max_{x\in[a,b]}|f(x)|$, which is a Banach space. Every Cauchy sequence in a Banach space is a convergent sequence. Consider the sequence of the partial sums of the series (11):

$$
\begin{aligned}
s_0 &= y_0 \\
s_1 &= y_0 + y_1 \\
s_2 &= y_0 + y_1 + y_2 \\
&\vdots \\
s_n &= y_0 + y_1 + y_2 + \cdots + y_n \\
&\vdots
\end{aligned}
$$

We have to show that the sequence of partial sums $\{s_n\}$ is convergent. We have

$$||s_{n+1} - s_n|| = ||y_{n+1}|| \le c||y_n|| \le c^2||y_{n-1}|| \le \cdots \le c^{n+1}||y_0||.$$

Using this relation and the triangle inequality, for $n, m \in \mathbb{N}$, with $n > m$, we get

$$
\begin{aligned}
&||s_n - s_m|| \\
&= ||(s_n - s_{n-1}) + (s_{n-1} - s_{n-2}) + \cdots + (s_{m+1} - s_m)|| \\
&\le ||s_n - s_{n-1}|| + ||s_{n-1} - s_{n-2}|| + \cdots + ||s_{m+1} - s_m|| \\
&\le c^n||y_0|| + c^{n-1}||y_0|| + c^{n-2}||y_0|| + \cdots + c^{m+1}||y_0|| \\
&= (c^n + c^{n-1} + c^{n-2} + \cdots + c^{m+1})||y_0|| \\
&= c^{m+1}\frac{1 - c^{n-m}}{1 - c}
\end{aligned}
$$

Since $0 \le c < 1$, then $\lim_{m\to\infty} ||s_n - s_m|| = 0$. Hence $\{s_n\}$ is a Cauchy sequence and therefore it is convergent. This means that the series (11) is convergent. This proves the theorem. □

4 Conclusion

In this paper, we tried to increase the radius of convergence for solutions to the the Lane-Emden equation. To do so, we examined the effect of increasing the order of non-linearity, M, as well as increasing the value imposed at the initial point, a. Further, we varied the linear operator used and studied the resulting effect. We observed that increasing M and a resulted in a larger interval of convergence for the solutions. Furthermore, we have found that the auxiliary parameter $\hbar$ in the homotopy equation not only provides for convergence of the solution, but also controls the radius of convergence.

Acknowledgment

Our undergraduate research team member recieved a partial financial grant from Rochester Institute of Technology.

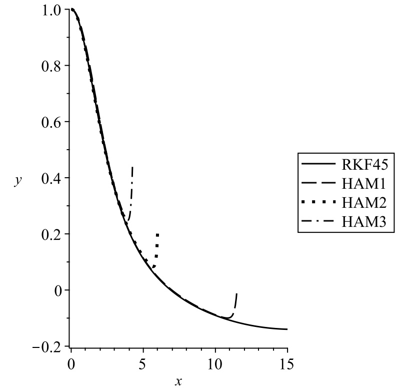

(a) Three HAM algorithms when $a = 1$

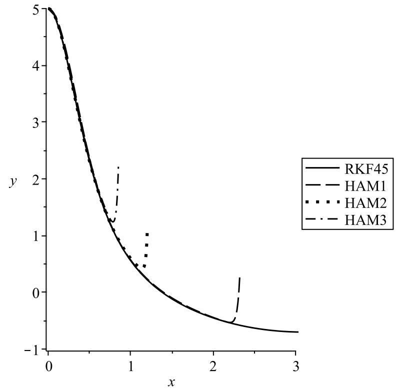

(b) Three HAM algorithms when $a = 5$

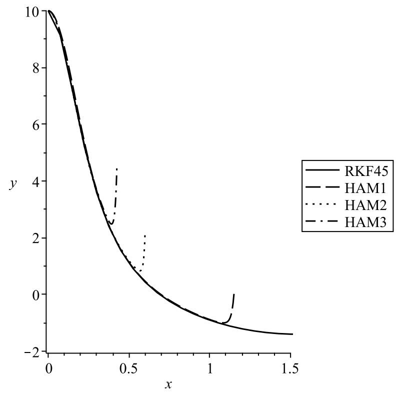

(c) Three HAM algorithms when $a = 10$

Fig. 6: Solution interval of convergence comparison between the three different homotopy constructions of 20^{th} order HAM series solution when $a = 1$ in (a), when $a = 5$ in (b) and when $a = 10$ in (c).

References

[1] F. Abbas and H. Eberl, Analytical substrate flux approximation for the Monod boundary value problem, Applied Mathematics and Computation, Vol. 218, No. 4, pp. 1484–1494 (2011).

[2] S. Abbasbandy, T. Hayat, A. Alsaedi, M.M. Rashidi, Numerical and analytical solutions for Falkner-Skan flow of MHD Oldroyd-B fluid, International Journal of Numerical Methods for Heat & Fluid Flow, Vol. 24, No. 2, pp. 390–401 (2014).
[3] G. Adomian, R. Rach, N.T. Shawagfeh, On the analytic solution of the Lane-Emden equation, Foundations of Physics Letters, Vol. 8, No. 2, pp. 161–181 (1995).
[4] B.W. Carroll and D.A. Ostlie, An introduction to modern astrophysics, Cambridge University Press (2017).
[5] S. Chandrasekhar, An introduction to the study of stellar structure, Courier Corporation, Vol. 2, (1957).
[6] R. Emden, Gaskugeln: Anwendungen der mechanischen Wärmetheorie auf kosmologische und meteorologische Probleme, (1907).
[7] J.H. Lane, ART. IX.–On the Theoretical Temperature of the Sun; under the Hypothesis of a Gaseous Mass maintaining its Volume by its Internal Heat, and depending on the Laws of Gases as known to Terrestrial Experiment, American Journal of Science and Arts, Vol. 50, No. 57, pp. 1820-1879 (1870).
[8] S.J. Liao, Notes on the homotopy analysis method: some definitions and theorems, Communications in Nonlinear Science and Numerical Simulation, Vol. 14, No. 4, pp. 983–997 (2009).
[9] S.J. Liao, Beyond perturbation: introduction to the homotopy analysis method, CRC Press, (2003).
[10] S.J. Liao, A new analytic algorithm of Lane–Emden type equations Applied Mathematics and Computation, Vol. 142, No. 1, pp. 1–16 (2003).
[11] S.J. Liao, On the proposed homotopy analysis technique for nonlinear problems and its applications, Shanghai Jiao Tong University, Ph.D. thesis, (1992).
[12] J.I. Ramos, Series approach to the Lane–Emden equation and comparison with the homotopy perturbation method, Chaos, Solitons & Fractals, Vol. 38, No. 2, pp. 400–408 (2008).
[13] M.M. Rashidi, S. Abbasbandy et al., Analytic approximate solutions for heat transfer of a micropolar fluid through a porous medium with radiation, Communications in Nonlinear Science and Numerical Simulation, Vol. 16, No. 4, pp. 1874–1889 (2011).
[14] M. Sajid and T. Hayat and S. Asghar, Comparison between the HAM and HPM solutions of thin film flows of non-Newtonian fluids on a moving belt, Nonlinear Dynamics, Vol. 50, No. 1, pp. 27–35 (2007).
[15] Y. Tan, S. Abbasbandy, Homotopy analysis method for quadratic Riccati differential equation, Communications in Nonlinear Science and Numerical Simulation, Vol. 13, No. 3, pp. 539–546 (2008).
[16] R.A. Van Gorder and K. Vajravelu , Analytic and numerical solutions to the Lane–Emden equation, Physics Letters A, Vol. 372, No. 39, pp. 6060–6065 (2008).
[17] A.M. Wazwaz, Solving Two Emden-Fowler Type Equations of Third Order by the Variational Iteration Method, Applied Mathematics & Information Sciences, Vol. 9, No. 5, pp. 2429 (2015).
[18] A.M. Wazwaz, R. Rach, and J.S. Duan, Adomian decomposition method for solving the Volterra integral form of the Lane-Emden equations with initial values and boundary conditions, Applied Mathematics and Computation, Vol. 219, No. 10, pp. 5004–5019 (2013).
[19] A.M. Wazwaz, The Variational Iteration Method for Solving New Fourth-Order Emden–Fowler Type Equations, Chemical Engineering Communications, Vol. 202, No. 11, pp. 1425–1437 (2015).
[20] A.M. Wazwaz, A reliable treatment of singular Emden-Fowler initial value problems and boundary value problems, Applied Mathematics and Computation, Vol. 217, No. 24, pp. 10387–10395 (2011).
[21] A.M. Wazwaz, The variational iteration method for solving systems of equations of Emden-Fowler type, Int. J. Comput. Math., Vol. 88, No. 16, pp. 3406–3415 (2011).
[22] A.M. Wazwaz, Adomian decomposition method for a reliable treatment of the Emden-Fowler equation, Applied Mathematics and Computation, Vol. 161, No. 2, pp. 543–560 (2005).
[23] A.M. Wazwaz, A reliable treatment of singular Emden-Fowler initial value problems and boundary value problems, Applied Mathematics and Computation, Vol. 217, No. 24, pp. 10387–10395 (2011).
[24] A.M. Wazwaz and R. Rach, Comparison of the Adomian decomposition method and the variational iteration method for solving the Lane-Emden equations of the first and second kinds, Kybernetes, Vol. 40, No. 9/10, pp. 1305–1318 (2011).
[25] A.M. Wazwaz, R. Rach, L. Bougoffa, J.S. Duan, Solving the Lane–Emden–Fowler type equations of higher orders by the Adomian decomposition method, Comput. Model. Eng. Sci.(CMES), Vol. 100, No. 6, pp. 507–529 (2014).

Fazal Abbas has a doctorate in Mathematical Biology from the University of Guelph, Guelph ON Canada. Dr. Abbas is passionate about mathematical modeling in various disciplines of life. His PhD results facilitated environmental engineers to develop biofilm-based wastewater treatment based technology. His current research interests are mathematical biology, mathematical finance, mathematical physics, convergent series solutions, dynamical systems and differential equations.

Petko Kitanov received PhD degree in Applied Mathematics from the University of Guelph, Canada. He was a postdoctoral researcher at the University of Ottawa and the University of Guelph. Now he is a visiting lecturer at Rochester Institute of Technology. He taught various math courses in different universities in Bulgaria, University of Limerick, Ireland, and the University of Ottawa and the University of Guelph in Canada. His interests are in differential equations, dynamical systems, nonlinear analysis, mathematical physics, and mathematical biology. He has published research papers in reputed international journals.

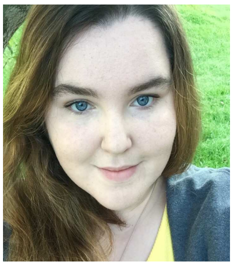

Shoshanna Longo is an undergraduate student majoring in Computer Engineering (BA) from Kate Gleason College of Engineering and minoring in applied mathematics at Rochester Institute of Technology. She has been researching the field of applied mathematics for three years with her main focus on the homotopy analysis method, Lane-Emden equation, the adomian decomposition method, nonlinear differential equations, and stellar structures. She presented the results in this paper at the undergraduate poster session at the January 2018 Joint Math Meetings.